CHARACTERIZATION OF A FULLY-INTEGRATED PERMANENT-MAGNET TURBINE GENERATOR

Bernard C. Yen[1], Florian Herrault[3], Keithan J. Hillman[4], Mark G. Allen[3], Fredric F. Ehrich[2], Stuart Jacobson[2], Chang-Hyeon Ji[3], Jeffrey H. Lang[1], Hanqing Li[2], Zoltan S. Spakovszky[2], and David R. Veazie[4]

[1]EECS, Massachusetts Institute of Technology, Cambridge, MA, USA
[2]Aero-Astro, Massachusetts Institute of Technology, Cambridge, MA, USA
[3]ECE, Georgia Institute of Technology, Atlanta, GA, USA
[4]ME, Clark Atlanta University, Atlanta, GA, USA

Abstract: This paper presents the design, fabrication, and testing of a fully-integrated permanent-magnet turbine generator based on silicon MEMS fabrication technology. This is the first silicon turbine generator supported by gas thrust and journal bearings experimentally shown to generate milliwatt-level power. In this device, a free-standing, 12 mm diameter magnetic rotor is spun above microfabricated copper windings having connectors threaded through the device. To date, the generator has delivered 19 mW to matched resistive loads of 0.33 Ω at a rotational speed of 40 krpm.

Key words: turbine generator, fully-integrated design, permanent-magnet machine, gas bearings

1. INTRODUCTION

The power density available from batteries is increasingly becoming a limiting factor in the capabilities of portable electronics. As a result, there is a growing need for compact, high power density sources. Microscale, axial-flux, permanent-magnet generators have been actively researched for use as a portable power source due to their high output power capabilities when operated at high speeds [1]. Miniaturization of generators is advantageous due to the cube-square law –weight scales with volume while power scales with surface area.

Previous millimeter-scale permanent-magnet generators may be broadly categorized into devices requiring an externally-driven spindle and others that are fully-integrated with both turbomachinery and supporting bearings. The fully-integrated devices reported thus far are not silicon-based and do not solely utilize gas bearings, two features that facilitate integration with a high-temperature, high-pressure gas turbine. Raisigel *et al*. demonstrated that an 8 mm diameter magnetic rotor cut using electric discharge machining from either bulk SmCo or NdFeB and supported by a magneto-pneumatic bearing produced 14.6 mW at 58 krpm [2]. Holmes *et al*. showed that a polymer-based axial-flux magnetic rotor, 7.5 mm in diameter, generated 1.1 mW at a rotational speed of 30 krpm [3]. This rotor was supported by ball bearings. More recently, Herrault *et al*. fabricated and tested an air-driven, fully-integrated generator capable of generating 0.8 mW at a rotational speed of 203 krpm. The 2 mm diameter rotor for this generator was polymer-based and also supported by high-speed ball bearings [4]. In contrast, the integrated silicon generator described here contains air bearings and seals capable of providing axial and radial stiffness while avoiding dynamic coupling effects [5-6].

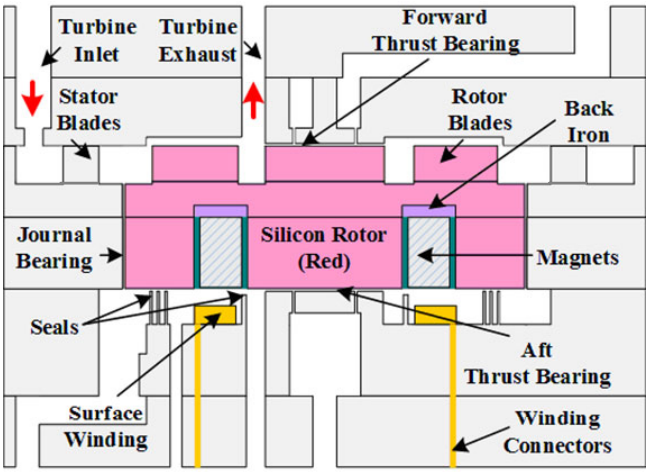

Fig. 1: Cross-sectional schematic of the fully-integrated permanent-magnet turbine generator. The device is constructed on a seven-wafer silicon stack.

2. DEVICE DESIGN AND FABRICATION

The generator studied here is a three-phase, eight-pole, axial-flux, synchronous machine fabricated from seven silicon wafers, with the first five fusion-bonded

to form the upper die and the remaining two fusion-bonded to form the bottom die. Magnetics and windings are integrated after the silicon structure is completed. As shown in Figs. 1-3, the device contains a free-standing silicon rotor enclosed by axial gas thrust bearings and a radial gas journal bearing.

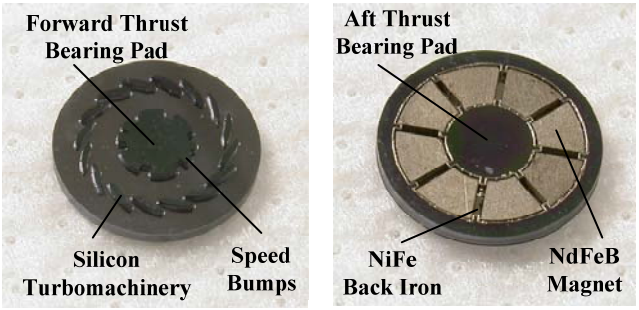

(a) Forward side *(b) Aft side*

Fig. 2: Forward and aft side of the fully-integrated silicon magnetic rotor.

A drop-in scheme is used to construct the magnetic silicon rotor, 12 mm in diameter and 1.28 mm thick. The silicon rotor is fabricated with a 600 μm deep annular cavity having an inner radius of 2.5 mm and an outer radius of 5.0 mm. Eight permanent magnet pieces are cut using laser-machining from a 500 μm thick sheet of NdFeB material. Separately on another silicon wafer, eight 50 μm thick NiFe back iron pieces are electroplated, released, and cleaned. Prior to rotor assembly, all the magnet and back iron pieces are weighed, and the arrangement that results in the least rotor imbalance — the distance between the geometric center and the center of mass — is determined. Ring magnet and back iron are not used because they cannot be easily centered and balanced; the journal bearing requires a rotor with minimal imbalance. Using commercially available super glue gel SGG2, the back iron pieces are glued down first, followed by the magnet pieces, which are staggered 22.5^{o} from the back iron to establish a continuous magnetic circuit.

The drop-in scheme is also applied to the lower die. Three-phase, eight-pole copper surface windings with three turns per pole are electroplated on a separate, oxidized silicon substrate. The surface winding consists of two copper layers, each approximately 100 μm thick, sandwiching a via layer. The bottom layer is electroplated from a 3000 Å copper seed layer using SU-2025 as a mold. Following this, a copper via layer is electroplated, again using SU-2025 as a mold. A second seed layer is deposited above the via layer for electroplating the top layer using NR2-2000 as the mold. Upon completion, the NR2-200 mold is removed, and the winding is released using HF. Six electrical connectors, bent 90^{o} toward the aft side prior to insertion, are threaded through mating holes on the silicon structure, and super glue is applied to the aft side of the winding to affix it to the silicon structure. As a final step, twelve 30 AWG wires — two per connector to allow simultaneous resistive loading and voltage probing — are soldered from the aft side of the device.

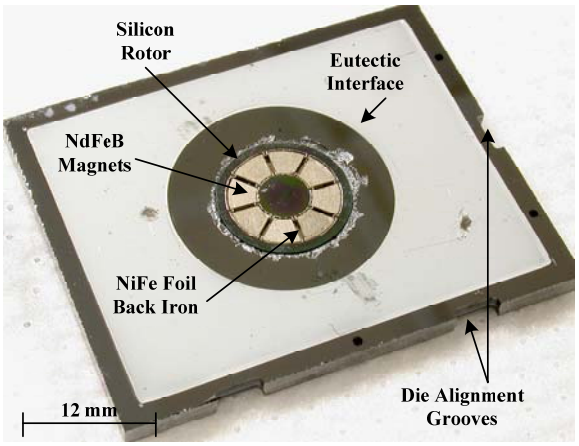

(a) Upper turbine generator die

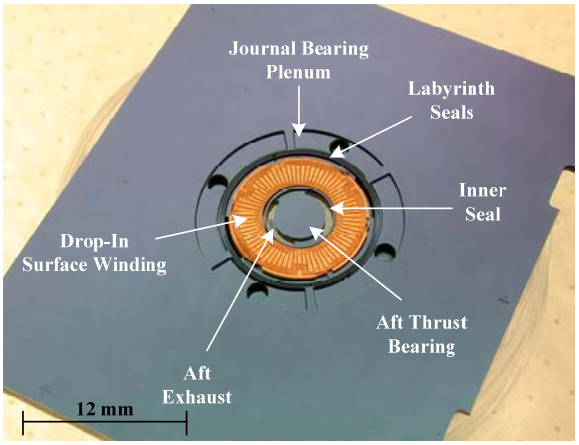

(b) Lower turbine generator die

Fig. 3: Fabricated magnetic generator dies. The upper die in Fig. 3(a) contains the rotor and the lower die in Fig. 3(b) contains the drop-in copper stator winding.

The upper and lower generator die are aligned under the microscope using built-in alignment markers and compressed inside an acrylic package, shown in Fig. 4. O-rings situated on the gas inlets to the device prevent leakage between the die and the package. An evaporated eutectic interface between the upper and lower dies, shown in Fig. 3(a), decreases leakage between the dies without the need for a permanent bond between the two halves. This enables multiple rotors to be tested in the same stator die.

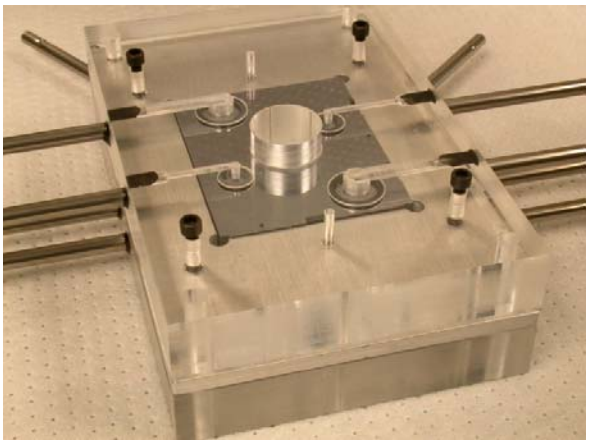

Fig. 4: Acrylic package with metal tabulations in which the magnetic generator is tested.

3. HYDROSTATIC GAS BEARINGS

The rotor containing the magnets is supported radially and axially by hydrostatic gas journal and thrust bearings respectively. The bearing design is based on previously established scaling laws, a new theory for micro-gas bearing dynamic behavior, and a first-of-a-kind criterion for whirl instability [5-6]. The damping ratio, natural frequency, and whirl instability limit are governed by the bearing geometry and fluid dynamic parameters. The key parameter that sets the bearing damping ratio, stiffness, and natural frequency is the bearing pressure difference, Δp. The theory shows that the natural frequency scales mainly with the square-root of Δp whereas the damping ratio scales with the inverse square-root of Δp. Flow in the bearing gap induced by the rotor motion sets up viscous stress and pressure fields that can give rise to whirl inducing bearing forces, leading to instability. This occurs at higher speeds and limits the stable operating range.

One of the major challenges encountered in the operation of the device is the ability to smoothly transition from subcritical to supercritical operation when accelerating to high speed. Since the natural frequency and damping ratio yield opposing trends as a function of Δp, the strategy is to initially set Δp to low values to yield a high damping ratio when crossing the natural frequency. Then the turbine pressure and Δp are increased in an alternating fashion to operate the rotor supercritically but below the whirl instability limit as shown in Fig. 5. The stable, supercritical operating region is bound by the dashed red line representing the whirl instability limit and the natural frequency marked by the solid black line.

A series of experiments were carried out to identify the natural frequency of the magnetic rotor and details can be found in [7]. The measured natural frequencies, marked in Fig. 5 by the black circles, show good agreement with the calculated values, validating the scaling laws and previously established models. This is the first time a MEMS fully-integrated permanent-magnet silicon turbine generator supported by gas bearings is operated at supercritical speeds. The rotor speed trace is marked by the red squares in Fig. 5.

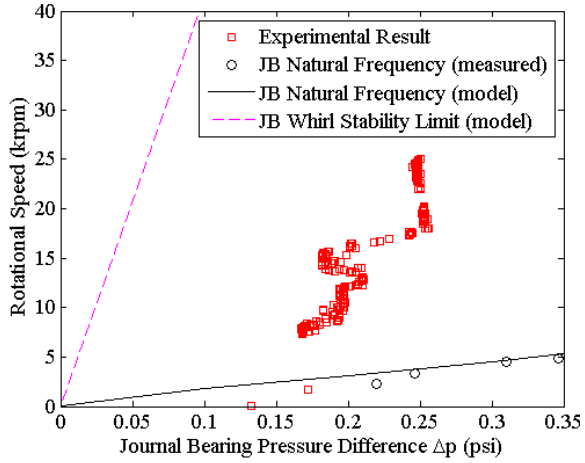

Fig. 5: Measured and computed natural frequency of magnetic rotor, and supercritical operation of device at 25 krpm. The standard deviation of error is 22 rpm for speed and 0.004 psi for Δp.

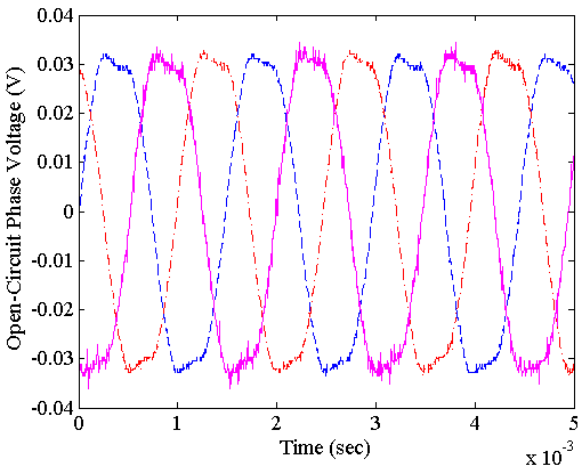

Fig. 6: Line-neutral open-circuit voltage at 10 krpm.

4. GENERATOR TESTING

To characterize the fully-integrated generator, both open-circuit and loaded tests are performed. For the open-circuit tests, BNC probes are connected to each of the three winding phases through the soldered wires. Fig. 6 shows the three-phase open-circuit voltage waveforms observed on the oscilloscope with the rotor

spinning at 10 krpm. Experimental phase voltage data as a function of rotational speed is shown in Fig. 7.

The loaded voltage and power characterizations are performed by connecting three load resistors of R_L = 0.33 Ω to the soldered wires, one per phase. The load is chosen to match the phase resistance, which maximizes the output power delivered. Note that the phase inductance is small and negligible. This condition is verified in Fig. 8, where the output power of the generator is measured for five resistor sets, and the highest measured power occurs for 0.33-Ω set. Fig. 7 shows that the loaded phase voltage is approximately half of the unloaded voltage, which further verifies the matched load condition. Fig. 7 also depicts the output power as a function of rotational speed; the maximum power achieved is 19 mW at a speed of 40 krpm, corresponding to a power density of 0.46 mW/mm^3. The phase voltage is linear with speed while the output power is quadratic with speed. Higher speeds could not be achieved due to flow leakage issues and structural integrity problems of the clamped device.

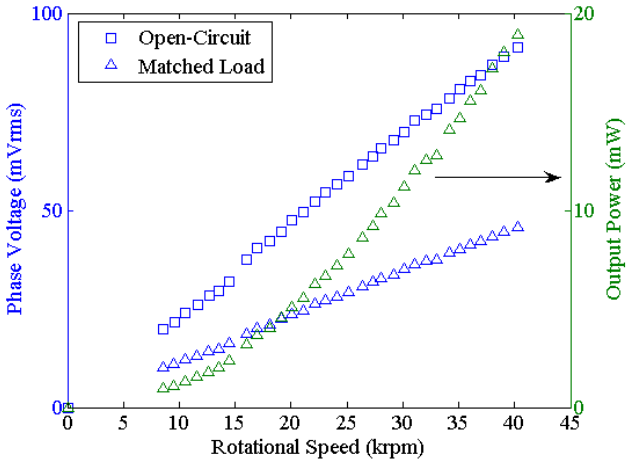

Fig. 7: Line-neutral phase voltage and three-phase power data for the fully-integrated silicon generator.

5. CONCLUSION

A fully-integrated silicon permanent-magnet turbine generator supported by gas bearings has been experimentally verified to generate 19 mW at 40 krpm rotor speed. This is the first time such a generator has produced net power. The fully-integrated device represents a major step toward the fabrication of a gas turbine generator powered by hydrocarbon fuel. Such a feat would result in a portable power source with high energy and power densities.

ACKNOWLEDGEMENT

All the silicon microfabrication work was performed at the MIT Microsystems Technology Laboratories. Funding for this work was provided by the Army Research Laboratory (DAAD19-01-2-0010) under the Collaborative Technology Alliance in Power and Energy program, managed by Mr. John Hopkins (ARL) and Dr. Mukund Acharya (Honeywell). The authors also wish to acknowledge Chiang Juay Teo for his help with the gas bearing design.

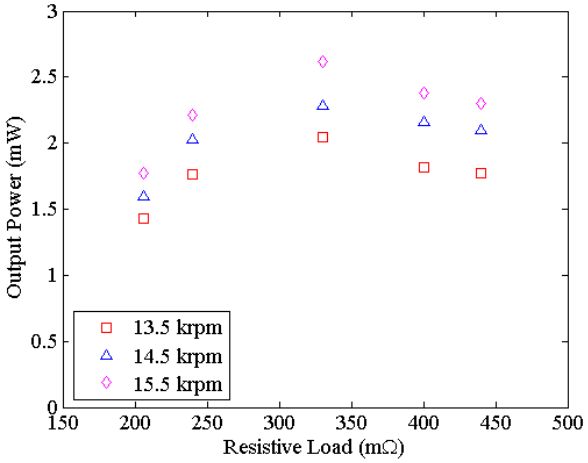

Fig. 8: Three-phase power delivered for various loads.

REFERENCES

[1] Arnold D P, Herrault F, Zana I, Galle P, Park J-W, Das S, Lang J H, Allen M G 2006 Design optimization of an 8 W, microscale, axial-flux, permanent-magnet generator *J. Micromech. Microeng.* **16** S290–S296

[2] Raisigel H, Cugat O, Delamare J 2006 Permanent magnet planar micro-generators *Sens. Actuators A* **130–131** 438–444

[3] Holmes A S, Hong G, Pullen K R 2005 Axial-flux permanent magnet machines for micropower generation *J. Microelectromech Syst.* **14** 54–62

[4] Herrault F, Ji C-H, Kim S-H, Wu X, Allen M G 2008 A microfluidic-electric package for power MEMS generators *Proc. 21st IEEE International Conference on Micro Electro Mech. Systems (Tucson, Arizona, 13–17 January 2008)* 112–115

[5] Spakovszky Z S, Liu L X 2005 Scaling laws for ultra-short hydrostatic gas journal bearings *J. Vib. Acoust. ASME* **127** 254–261

[6] Teo C J 2006 *MEMS turbomachinery rotordynamics: modeling, design, and testing* (Cambridge, MA, June 2006, MIT PhD Thesis)

[7] Yen B C 2008 *A fully-integrated multi-watt permanent-magnet turbine generator* (Cambridge, MA, September 2008, MIT PhD Thesis)